J Cerebral Blood Flow and Metabolism (2013)
doi: 10.1038/jcbfm.2013.155

IL-10 deficiency exacerbates the brain inflammatory response to permanent ischemia without preventing resolution of the lesion

Isabel Pérez-de Puig[1,2], Francesc Miró[2], Angélica Salas-Perdomo[1,2], Ester Bonfill-Teixidor[1,2], Maura Ferrer-Ferrer[2], Leonardo Márquez-Kisinousky[1], Anna M. Planas[1,2,*]

[1] Departament d'Isquèmia Cerebral i Neurodegeneració, Institut d'Investigacions Biomèdiques de Barcelona (IIBB), Consejo Superior de Investigaciones Científicas (CSIC), Barcelona, Spain.

[2] Institut d'Investigacions Biomèdiques August Pi i Sunyer (IDIBAPS), Barcelona, Spain.

*** Corresponding author:**

Anna M. Planas, PhD
IIBB-CSIC, IDIBAPS
Rosselló 161, planta 6
08036-Barcelona, Spain
E-mail: anna.planas@iibb.csic.es
Phone: +34-93 363 83 27
Fax: +34-93 363 83 01

Running Head: Stroke in IL-10 KO mice: Inflammation and outcome

Keywords: inflammation, stroke, myeloid cells, microglia, cytokines,

ABSTRACT

Stroke induces inflammation that can aggravate brain damage. This work examines whether interleukin-10 (IL-10) deficiency exacerbates inflammation and worsens the outcome of permanent middle cerebral artery occlusion. IL-10 and IL-10 receptor (IL-10R) expression increased after ischemia. From day 4, reactive astrocytes showed strong IL-10R immunoreactivity. IL-10 KO mice kept in conventional housing showed more mortality after pMCAO than the WT. This effect was associated to the presence of signs of colitis in the IL-10 KO mice, suggesting that ongoing systemic inflammation was a confounding factor. In a pathogen-free environment, IL-10 deficiency slightly increased infarct volume and neurological deficits. Induction of pro-inflammatory molecules in the IL-10 KO brain was similar to that in the WT 6 hours post-ischemia, but was higher at day 4, while differences decreased at day 7. IL-10 deficiency promoted the presence of more mature phagocytic cells in the ischemic tissue, and enhanced the expression of M2 markers and the T cell inhibitory molecule CTLA- 4. These findings agree with a role of IL-10 attenuating local inflammatory reactions, but do not support an essential function of IL-10 in lesion resolution. Up-regulation of alternative immunosuppressive molecules after brain ischemia can compensate, at least in part, the absence of IL-10.

Keywords: IL-10, inflammation, immunosupression, stroke, mouse

INTRODUCTION

Stroke induces inflammation that is considered detrimental in the acute phase. Insufficient oxygen supply triggers a transcriptional program designed to promote cellular adaptation to hypoxia [1,2]. Ischemic conditions can induce the expression of inflammatory mediators in microglia [3,4], and up-regulate the expression of toll-like receptors (TLR) [5] and other danger signal receptors [6]. Necrotic cell death induces secondary inflammatory reactions by liberating intracellular molecules to the extracellular environment [7] where they act as danger signals activating nearby glial cells. This process causes a second release of pro-inflammatory mediators [8] amplifying the initial inflammatory response to ischemia. Inflammatory mediators can be neurotoxic [9] and they induce chemoattraction of blood leukocytes, which, in turn, can release proteases and pro-oxidant agents further exacerbating the lesion [10]. However, the inflammatory reaction after acute brain damage is a complex dynamic process naturally set up to clear the necrotic tissue and evolving through various steps from initiation to resolution. Macrophages carry out an essential role in the process of tissue damage resolution by clearing dead cells and cell debris [11]. Although numerous molecules have been identified as players in the multifaceted inflammatory response to acute brain damage, more knowledge is needed to understand the critical molecules orchestrating its dynamics.

Interleukin-10 (IL-10) is a crucial anti-inflammatory cytokine that suppresses pro-inflammatory signals and immune responses. Several lines of evidence support that the cerebral expression of IL-10 is beneficial after experimental stroke as IL-10 transgenic mice over-expressing IL-10 in astrocytes, microglia, and endothelial brain cells showed smaller infarcts [12]. Furthermore, IL-10 gene transfer using adenoviral vectors reduced

infarct volume in a model of photothrombotic ischemia in rats [13]. Accordingly, mice deficient in IL-10 showed larger infarctions after permanent middle cerebral artery occlusion (pMCAO) [14]. In agreement with these findings, low levels of circulating IL-10 in patients with lacunar stroke were associated with a worse outcome [15]. Animals deficient in IL-10 lack the anti-inflammatory drive of this cytokine, and therefore provide a good model to test whether and how IL-10 is involved in stroke outcome. Here we studied the inflammatory response of IL-10 knockout (IL-10 KO) mice to brain ischemia to better understand the role of this molecule in acute brain damage.

METHODS

Animals

Animal work was carried out in agreement with the local regulations and in compliance with the Spanish Directives (Real Decreto 53/2013) that follow Directives of the European Community. Experimental procedures were approved by the Ethical Committee (CEEA) of the University of Barcelona (UB). IL-10 KO and wild type (WT) mice on a C57BL/10j background were obtained from the Jackson Laboratory. In an initial pilot study we found that some of the IL-10 KO mice kept under conventional animal house conditions developed signs of colitis. To avoid this pathology, IL-10 KO and WT mice were subjected to embryo transfer and were kept in a pathogen-free zone (SPF) in the animal house of the School of Medicine (UB). Under SPF conditions IL-10 KO mice did not develop overt signs of colitis at 3-4 months, in agreement with previous reports [16].

Brain ischemia

Permanent distal occlusion of the right middle cerebral artery (pMCAO) was carried out in adult (3-4 month) male WT (n=78) and IL-10 KO (n=68) mice under isoflurane

anaesthesia in 30 % O_2 and 70 % N_2O. After drilling a small hole in the cranium at the level of the distal portion of the MCA, the artery was occluded by cauterization. Flow obstruction was visually verified. Animals showing subdural haemorrhages or signs of incorrect surgery were immediately excluded from the study (less than 5 % in each group). After surgery, animals were allowed to recover from the anaesthesia and were returned to their cages.

Infarct volume by MRI

Infarct volume was assessed by MRI in a 7.0 T BioSpec 70/30 horizontal animal scanner (Bruker BioSpin, Ettlingen, Germany), equipped with a 12-cm inner diameter actively shielded gradient system (400 mT/m). The receiver coil was a phased array surface coil for mouse brain. Mice were placed in a supine position in a Plexiglas holder with a nose cone for administering anaesthesia (isoflurane in a mixure of 30% O_2 and 70% N_2O), fixed with a tooth bar, ear bars and adhesive tape and maintained under controlled temperature during the acquisition period. Tripilot scans were used for accurate positioning of the animal's head in the isocenter of the magnet. T2 relaxometry maps were acquired with a multi slice multi echo acquisition sequence with 16 effective echo times increasing from 11 to 176 ms, slice thickness= 0.5 mm, number of slices= 18, Repetition Time = 4764 ms, Field of view= 20 mm^3, matrix size 256 pixels and spatial resolution 0.078 mm^2/pixel. Data were processed using Paravision 5.0 software (Bruker). Infarct volume was calculated from the images using NIH Image-J software (http://rsb.info.nih.gov/ij). The area of infarction was measured in each brain slice and the total infarct volume was obtained by integration of the infarcted areas. A correction for edema was made in each area by multiplying the infarct area by the ratio of the contralateral to the ipsilateral hemisphere. Mice were scanned longitudinally at 1, 4 and

7 days, or only once before they were killed. Mice were assigned a code that did not reveal the identity of the groups and images were analyzed in a blind fashion.

Measurements of infarct volume after tissue histology

In a group of mice, infarct volume was determined by two methods, i.e. *in vivo* MRI at day 7 was followed by post-mortem histology in the same animals. After MRI, mice were anesthetized and transcardially perfused with saline followed by 4% paraformaldehyde. Brains were fixed overnight with this fixative, washed in phosphate buffer, cryoprotected in 30% sucrose and frozen. Serial coronal brain sections were obtained every 500 μm in a cryostat. After cresyl violet staining, the area of infarction in each section was measured using Image-J software. Areas were integrated to calculate infarct volume.

Assessment of brain edema

The brain water content was measured 4 days after pMCAO using the wet/dry weight method. The cerebellum was excluded and the forebrain was divided in the two hemispheres (ipsilateral and contralateral). The two brain pieces were immediately weighed (wet weight), dehydrated at 65 ºC for 72 hours and reweighed (dry weight). The difference between wet and dry weight was normalized to the initial size of the tissue by dividing by the corresponding wet weight value. The ratio between the ipsilateral and contralateral water content was calculated and values are expressed as the percentage of increase in tissue water content induced by ischemia.

Behavioural test

At day 3, the adhesion/removal tape test that evaluates sensorimotor deficits was carried out as previously described [17]. Briefly, an adhesive tape is placed in one of the forelimbs. The animal naturally tries to remove it and the time duration of the following

three steps is measured: time of forelimb shaking, time until contact with the mouth, and time until tape removal. Animals were trained the two days prior to ischemia.

Microglia cultures

Microglial cultures were obtained from the cerebral cortices of 1-day-old neonatal mice (Supplementary Materials) [8]. Cells were subjected to ischemic conditions for 3 hours in an anoxia incubator (GalaxyR/RS Biotech, New Brunswick, Eppendorf, Enfield, CT, USA) containing an atmosphere of 95 % N_2, and 5 % CO_2 at 37 ºC, and they were kept for 3 hours more under normoxic conditions. Other cells were exposed to 10 ng/mL lypopolysaccharide (LPS) (Escherichia coli 055:B5) (Sigma-Aldrich) for 6 hours. Ten ng/mL recombinant murine IL-10 (#210-10, PreproTech, Rocky Hill, NJ, USA) was added to the cell cultures 30 min before the above challenges.

qRT-PCR

Total RNA was extracted using Purelink RNA Kit (Invitrogen, Spain). RNA quantity and purity were determined using ND-1000 micro-spectrophotometer (NanoDrop Technologies, Wilmington, DE, USA). One-µg total RNA was reverse-transcribed using a mixture of random primers (High Capacity cDNA Reverse Transcription kit, Applied Biosystems). TaqMan^R primer sequences were used to evaluate the expression of IL-10 (Mm00439614_m1) and CTLA-4 (Mm00486849_m1) mRNA (Life Technologies). Quantification was carried out by normalizing Ct (Cycle threshold) values with Ct of the TaqMan^R primer sequence for glyceraldehyde 3-phosphate dehydrogenase (GAPDH) (Mm99999915_g1), and data were analyzed with the 2-$\Delta\Delta$CT method. The rest of PCR primers (see list in Supplementary Table 1) were designed with Primer3 software to bridge the exon–intron boundaries within the gene of interest to exclude amplification of contaminating genomic DNA. Primers were purchased from IDT (Laboratorios Conda

S.A., Torrejon de Ardoz, Spain). Real-time quantitative RT-PCR analysis was carried out by SYBR green I dye detection (#11761500, Invitrogen) using the iCycler iQTM Multicolor Real-Time Detection System (Bio-Rad, Hercules, CA, USA). Optimized thermal cycling conditions were: 1 min at 50 ºC, 8 min and 30 sec at 95 ºC and 40 cycles of 15 sec at 95 ºC and 30 sec at 60 ºC. Data were collected after each cycle and were graphically displayed (iCycler iQTM Real-time Detection System Software, version 3.1, Bio-Rad). Melt curves were performed upon completion of the cycles to ensure specificity of the product amplification. Housekeeping gene for normalization was succinate dehydrogenase complex subunit A (SDHA). Quantification was carried out using the standard dilution calibration curve and values were normalized to the reference gene. For comparison purposes, values of all samples are expressed as fold versus the mean (n=3-6) control value.

ELISA immunoassays

The concentration of cytokines and chemokines in plasma was analyzed with Q-Plex™ Mouse Array IR assays (#130951MS, Quansys Bioscience, Logan, Utah, USA) and measures were obtained in an Odissey system (LI-COR, Lincoln, NE, USA). Conventional ELISA assays were carried out to measure the concentration of soluble IL-10 (#88-7104, eBioscience, San Diego, CA, USA) in brain tissue extracts that were obtained as described [18]. Tumor necrosis factor-α (TNF-α) (#88-7324-88, eBioscience) and IL-6 (#861.020.005, Diaclone, San Diego, CA, USA) were measured in the medium of cultured microglia.

Isolation of cells from tissues

Ischemic (4 days after pMCAO) (WT n=10 and IL-10 KO n=10) mice and controls (n=6 WT and n=6 IL-10 KO) were anesthetized and transcardially perfused with 40 mL saline. The ischemic parietal cortex (ipsilateral) and the corresponding cortex of the non-ischemic

hemisphere (contralateral) were dissected out and analysed separately. The dissected contralateral or ipsilateral regions of two mice were pooled together and incubated for 30 minutes at 37°C in 5 mL of RPMI 1640 medium (Life Technologies S.A., Alcobendas, Madrid, Spain) containing 100 U/mL collagenase IV and 50 U/mL DNAse I, and pressed through a cell strainer (40 µm; BD Biosciences, San Jose, CA, USA). Cells were recovered after centrifugation at 400 x*g* for 10 min and separated from myelin and debris in 70 % and 30 % isotonic Percoll gradient (GE Healthcare) prepared in Hank's Balanced Salt Solution (HBSS) without calcium or magnesium. Samples were centrifuged at 1,000 x *g* for 30 min without acceleration or brake. Cells were collected from the interface, washed once with HBSS, and processed for flow cytometry.

Spleens were obtained 4 and 7 days after pMCAO. They were dissected in 1 ml RPMI 1640 medium and pressed through a 40 µm cell strainer (BD Biosciences). Cells were incubated for 5 min in red blood cell lysis buffer (150 mM NH_4Cl, 10 mM $KHCO_3$, 0.1 mM EDTA) and washed twice in PBS.

Flow cytometry

Isolated brain cells were washed with fluorescence-activated cell sorting (FACS) buffer (phosphate-buffered saline, 2 mM EDTA, 2% FBS), incubated at 4 ºC for 10 min with FcBlock (1/200; Clone 2.4G2; BD Pharmingen), and incubated with primary antibodies in FACS buffer for 30 min at 4ºC. The antibodies used were rat anti-mouse CD11b (clone M1/70, Alexa Fluor 647, BD Pharmingen), CD45 (clone 30-F11, FITC, BD Pharmingen), F4/80 Pan macrophages (clone BM8, FITC, Hycult Biotec, Uden, The Netherlands), Ly6G (clone 1A8, PE-Cy7, BD Pharmingen). Isotype controls were rat IgG2bκ (clone A95-1, Alexa Fluor 647 or FITC, BD Pharmingen), rat IgG2a (FITC, Hycult Biotech), and rat IgG2aκ (clone R35-95, PE-Cy7, BD Pharmingen). Data acquisition was carried out in a BD FacsCantoII cytometer (BD Biosciences) using the FacsDiva software (BD Biosciences).

Cells were morphologically identified by linear forward scatter (FSC-A) and side scatter (SSC-A) parameters (Supplementary Fig. 1). Data analysis was performed with FlowJo software (version 7.6.5, TreeStar Inc., Ashland, OR, USA). Again, cells were plotted on forward versus side scatter and single cells were gated on FSC-A versus FSC-H linearity. Flow-Count Fluorospheres (Beckman-Coulter) were used for absolute quantification.

Splenocytes were incubated in FACS buffer with FcBlock for 10 min at 4 ºC and then with the following antibodies for 30 min at 4 ºC: armenian hamster anti-mouse CD3 (clone 145-2C11, Brilliant Violet-421, BioLegend), rat anti-mouse CD4 (clone GK1.5, FITC, AbDserotec), armenian hamster anti-mouse CD152 (clone UC10-4B9, PE, BioLegend), and rat anti-mouse CD25 (clone PC61, Alexa Fluor-647, AbDserotec). After surface staining, cells were prepared for intracellular staining by fixation for 20 min and permeabilization for 20 min. Fixation and permeabilization buffers were from eBioscience. Cells were then incubated for 30 min with rat anti-mouse Foxp3 (clone FJK-16s, PE-Cy7, eBioscience) antibodies. Isotype controls were Armenian hamster IgG (clone HTK888, Brilliant Violet 421 or PE, BioLegend), rat IgG2bκ (clone A95-1, FITC or Alexa Fluor-647, BD Pharmingen), and rat IgG2aκ (clone R35-95, PE-Cy7, BD Pharmingen). Data were acquired and analyzed as indicated above.

Immunofluorescence

Cryostat brain sections (14 μm-thick) were fixed with acetone, blocked with rabbit serum and incubated overnight at 4ºC with a rabbit polyclonal primary antibody against IL-10R (#C-20; Santa Cruz Biotechnology Inc., CA, USA) diluted 1:100. Then, sections were incubated for 2 hours at room temperature with a secondary anti-rabbit antibody (Alexa Fluor-488, Molecular Probes®). Double immunostaining was carried out with a mouse monoclonal antibody against GFAP conjugated with Alexa Fluor-546 (#8152, Cell

Signalling Technology, Danvers, MA, USA) diluted 1:50, or with biotin-conjugated tomato isolectin (#L0651, Sigma) followed by incubation with Alexa Fluor-546 streptavidin (#S11225, Molecular Probes®). Sections were counterstained with Hoechst to visualize the cell nuclei and they were observed under a confocal microscope (Leica SP5).

Statistical analyses

Statistics were carried out using GraphPad software (GraphPad Software Inc., La Jolla, CA, USA). One-way ANOVA was used for comparisons between multiple groups followed by the post-hoc Bonferroni test. Two-way ANOVA was used for comparisons by genotype and by either brain hemisphere (ipsilateral/contralateral) or by time. Linear regression analysis was used for correlation studies. Sample size for infarct volume measures was calculated taking into account the known SD of the researcher that carried out the ischemia model.

RESULTS

pMCAO induces the expression of IL-10 and IL-10 receptor in brain tissue of WT mice

The expression of IL-10 mRNA progressively increased in the ipsilateral cortex of WT mice after pMCAO (Fig. 1A). The magnitude of IL-10 mRNA expression was positively correlated ($p<0.03$) to infarct volume, as assessed by MRI in the same animals, 6 hours (Fig 1B) and 7 days (Supplementary Fig. 2A) after pMCAO, suggesting that it was dependent on the severity of ischemia. A previous study showed that the numbers of cells expressing IL-10 mRNA in the ischemic tissue were correlated with the size of the lesion form 6 hours to 6 days after pMCAO in rats [19]. The presence of soluble IL-10 protein in the tissue also increased after ischemia, as assessed by ELISA (Fig. 1C). However, this parameter was not significantly correlated with infarct volume at day 4

(Supplementary Fig. 2B) showing some dissociation between the post-ischemic induction of IL-10 mRNA and the tissue concentration of IL-10.

pMCAO also up-regulated the expression of IL-10 receptor (IL-10R) mRNA, but strong increases were not detected until day 4 (Fig. 1D). Immunofluorescence against IL-10R showed no immunoreactivity in the control cortex (Fig. 1E). One, 4 and 7 days post-ischemia, IL-10R immunoreactive cells were occasionally seen in the subarachnoid space on the surface of the infarcted cortex (Fig. 1F, Supplementary Fig. 2C). However, it was not until day 4 that the expression of IL-10R was strongly up-regulated in reactive astrocytes of cortical layers I and II within the infarcted zone and at the subpial glia limitans (Fig. 1G,H). Isolectin positive myeloid cells immunoreactive for IL-10R were only occasionally detected (Fig. 1G). These results show that reactive astrocytes are strongly receptive to IL-10 and might be involved in modulating inflammatory and immune responses after stroke.

IL-10 deficiency slightly increases lesion volume and neurological deficits after pMCAO

Focal ischemia by distal pMCAO in C57 mice causes a lesion restricted to a portion of the cortical MCA territory (mainly the parietal cortex) (Fig. 2A). pMCAO did not cause mortality within the first 7 days, neither in WT mice nor in IL-10 deficient mice that were housed in SPF. However, in a preliminary experiment carried out in animals maintained under conventional housing conditions (not SPF) (WT n=9, IL-10 KO n=8) we observed no mortality in WT mice but 50 % mortality in the IL-10 KO mice within 7 days after pMCAO (Chi-square=5.88, $p<0.05$). IL-10 KO mice are known to spontaneously develop colitis when they are kept under conventional animal housing conditions [16]. Post-stroke mortality in the IL-10 KO mice was associated to the presence of overt signs of colitis as assessed after visual observation of variable degrees of rectal prolapse, which

demonstrates a rather severe colitic condition. Furthermore, IL-10 KO mice housed in the conventional animal house had smaller ($p<0.001$) body weight (mean ± SD, n) (16.7 ± 3.1 g, n=9) than the WT mice (27.5 ± 2.5 g, n=10) housed in the same conditions. This effect was not observed in IL-10 KO mice (27.8 ± 3 g, n=51) and WT mice (29.1 ± 3.8 g; n=45) housed in SPF. The finding that the presence of pathogens and ongoing peripheral inflammation in the IL-10 KO mice increased stroke mortality is in agreement with the notion that systemic inflammation aggravates stroke outcome [20]. In order to explore the consequences of IL-10 deficiency in the stroked brain without confounding systemic inflammatory pathology, the following experiments were carried out after the mouse colonies (both IL-10 KO and WT mice) were transferred to a SPF environment. The concentration of pro-inflammatory cytokines in the plasma of IL-10 KO and WT mice (naïve and 6 hours after pMCAO) that were kept in SPF conditions was examined to verify the absence of signs of subclinical inflammatory pathology (Supplementary Fig. 3).

The progression of brain damage was assessed in IL-10 KO and WT mice by carrying out a longitudinal MRI study at days 1, 4 and 7 after pMCAO using T2 relaxometry maps (Fig. 2A). IL-10 deficiency increased the size of the MRI lesion, but group differences were small and they were at the limit of statistical significance (two-way ANOVA by genotype and time, $p=0.049$ for genotype effect, and $p<0.001$ for time effect) (Fig. 2B). The maximal infarct volume increase versus WT was 16 % at day 4. Notably, IL-10 deficiency did not impair the process of involution of the MRI lesion, since infarct volume decreased at day 7 in both WT and IL-10 KO mice (Fig. 2B). A successive reduction of infarct volume within the first two weeks after pMCAO has been previously reported in this experimental stroke mouse model [21,22]. However, the histopathological and molecular correlates of lesion involution in this experimental pMCAO model in mice are not known. For histological validation of the MRI findings, we carried out ischemia in an additional

group of WT mice and IL-10 KO mice to evaluate infarct volume *in vivo* by MRI at day 7 followed by histological evaluation in the same mice (Fig. 2C). The correlation between MRI infarct volume and the corresponding histology volume was very good (linear regression r^2=0.8, p<0.001) (Fig. 2D). Two-way ANOVA by genotype and volume method (MRI versus histology) showed no significant effect of genotype but a significant effect of the volume method (p<0.001) due to smaller infarct volumes detected by histology (Fig. 2E). This effect was attributable to post-mortem and post-processing brain volume changes and to larger errors when estimating the distance between sections after cryostat sectioning than after *in vivo* MRI, where slice thickness and distance between sections are precisely and automatically set.

To assess whether the degree of edema within the first few days post-ischemia and the extent of shrinkage of the damaged tissue at later time points were different in the WT and IL-10 KO groups, we measured the ratio of the ipsilateral versus the contralateral MRI hemispheric brain volumes. At day 1, the volume of the ipsilateral hemisphere was larger than that of the contralateral hemisphere due to edema (Fig. 2F). This increase was attenuated at day 4, but at day 7 the volume of the ipsilateral hemisphere was smaller than that of the contralateral hemisphere due to tissue loss (Fig. 2A, F). However, these changes in brain volume were similar in the WT and IL-10 KO groups (Fig. 2F), suggesting that the absence of IL-10 interfered neither with ischemia-induced edema nor with lesion involution. In support of these findings, measures of brain water content at day 4 using the wet/dry weight method showed that ischemia increased the water content in the ipsilateral versus the contralateral hemisphere by (mean±SD) 0.98 ±0.27 % and 0.92± 0.37 % in WT (n=5) and IL-10 KO (n=2) groups, respectively.

pMCAO induced only mild neurological deficits that could be detected by the adhesion/removal tape test, which evaluates sensorimotor alterations, but not by the neurological score tests [23] often used in models of transient intraluminal MCAO (not shown). The neurological deficit observed with the adhesion/removal tape test was greater in IL-10 KO mice than in WT mice. The test showed a worse performance of the contralateral forepaw (left) in IL-10 KO mice 3 days after pMCAO (Fig. 2 G-I). However, at day 7, the worsening effect of IL-10 deficiency was attenuated (Fig. 2 G-I), supporting that the effects of IL-10 were mainly manifested during the first days after stroke.

IL-10 deficiency did not impair the cerebral inflammatory response early after pMCAO

We examined the inflammatory response in brain tissue early (6 hours) after pMCAO by measuring the mRNA expression of several cytokines, chemokines, adhesion molecules, and other inflammatory molecules with qRT-PCR. In WT mice, ischemia induced the expression of cytokines, such as tumor necrosis factor-α (TNF-α), IL-1β, and IL-6, as well as other inflammatory mediators, such as TLR-4, matrix metalloproteinase-9 (MMP-9), cyclooxygenase-2 (COX-2), and inducible nitric oxide synthase (iNOS) (Fig. 3). Ischemia also upregulated the mRNA expression of chemokines: monocyte chemoattractant protein-1 (MCP-1 or CCL2), neutrophil-activating protein KC (CXCL1), and macrophage inflammatory proteins MIP-1α (CCL3) and MIP-2α (CXCL2); the intercellular adhesion molecule-1 (ICAM-1); and growth factors, such as transforming growth factor-β (TGF-β), and insulin growth factor-1 (IGF-1) (Fig. 3). IL-10 deficiency showed a non-significant tendency to increase the expression of some of the above molecules in the ischemic tissue, while it induced a slightly lower expression of IL-6 and CXCL1 mRNA compared to that in WT mice (Fig. 3). Therefore, IL-10 deficiency did not significantly exacerbate the initial inflammatory reaction of resident cells within the first few hours following

pMCAO. The inflammatory reaction [24] to ischemia does not appear to be strongly regulated by IL-10 within the first hours after stroke onset.

To examine the direct anti-inflammatory effect of IL-10 we carried out an *in vitro* study in primary cultures of murine microglia. Cultured microglia (Fig. 4) exposed to ischemic conditions showed increased expression of pro-inflammatory cytokines like TNF-α (Fig. 4A, G), IL-6 (Fig. 4C, I), and IL-1β (Fig. 4E) 6 hours later. Notably, treatment with recombinant IL-10 did not prevent this inflammatory reaction (Fig. 4A, C, E, G, I). In contrast, treatment with IL-10 strongly suppressed the inflammatory response of microglia stimulated with LPS (Fig. 4B, D, F, H, J), showing that IL-10 effectively blocked the response to stimuli inducing activation of TLR-4 but not to lack of oxygen.

IL-10 deficiency induces an exaggerated inflammatory response 4 days after pMCAO

In contrast to the findings 6 hours post-ischemia, at 4 days a significantly higher mRNA expression of TNF-α, IL-1β, IL-6, TLR-4, MMP-9, Cox-2, ICAM-1, MCP-1, CXCL1, and MIP-1α was found in the ipsilateral cortex of IL-10 KO mice versus the WT (Fig. 5). Also, expression of iNOS and MIP-2α mRNA tended to be higher in IL-10 KO mice, but differences were not statistically significant (Fig. 5). In contrast to the above increases, the expression of CX3CL1, which is mainly produced by neurons, was reduced in the ipsilateral cortex of IL-10 KO mice versus the WT (Fig. 5). In addition, small increases in several molecules (IL-1β and MCP-1 mRNA) were detected at day 4 in the contralateral cortex of IL-10 KO mice versus the WT (Fig. 5), suggesting that IL-10 might prevent secondary inflammation in remote brain regions too. The finding of more pronounced inflammatory responses in the IL-10 KO brain at day 4 after ischemia is in agreement with the observation that expression of IL-10 and IL-10R was strongly up-regulated at this time point (Fig. 1).

Differences in the inflammatory response of IL-10 KO and WT mice are reduced at day 7

Differences between WT and IL-10 KO groups for the mRNA expression of several pro-inflammatory molecules, such as TNF-α, IL-1β, IL-6, TLR-4, MCP-1 and MMP-9 (Fig. 6), were no longer statistically significant seven days post-ischemia. However, MIP-2α and Cox-2 mRNA was higher in the IL-10 KO mice than in the WT, and an increase in Cox-2 expression also became apparent in the contralateral hemisphere compared with the corresponding WT (Fig. 6). At this time point, the mRNA expression of molecules involved in repair mechanisms [11], such as TGF-β and IGF-1, had increased versus previous time points, but this effect was similar in WT and IL-10 KO mice (Fig. 6), indicating that resolution of inflammation progressed also in the absence of IL-10.

Suppressive mechanisms are up-regulated in the IL-10 KO mice after pMCAO

The numbers and features of myeloid cells found in brain tissue of IL-10 KO and WT mice were examined by flow cytometry 4 days after pMCAO. The relative proportion of cells corresponding to microglia ($CD11b^{Dim}CD45^{low}$) decreased in the ischemic tissue of both IL-10 KO and WT mice compared to the contralateral hemisphere or the control brain (Supplementary Fig. 4). This effect was due to the presence of leukocytes ($CD45^{High}$) in the ischemic brain (Supplementary Fig. 4). However, the numbers of leukocytes, both $CD11b+CD45^{High}$ (myeloid cells) and $CD11b-CD45^{High}$ (lymphocytes), were similar in IL-10 KO and WT mice (Supplementary Fig. 4). Likewise, no differences in the number of F4/80+ cells (a marker of phagocytic microglia/macrophages) were found between the two genotypes (Fig. 7A). Nevertheless, IL-10 deficiency induced a shift in the phenotype of these cells due to the presence of significantly higher proportions and numbers of $F4/80^{High}$ cells in the ischemic tissue of IL-10 KO mice than in the WT, while this specific myeloid subpopulation was absent in the contralateral cortex or in controls (Fig. 7A).

F4/80^{High} cells are considered mature macrophages undergoing terminal differentiation in the tissue microenvironment [25]. Since F4/80^{High} cells are phagocytic cells that are expected to actively participate in clearing the damaged tissue, we examined the expression of galectin-3, which in macrophages plays a critical role in phagocytosis. Higher galectin-3 mRNA expression was detected in the ischemic tissue of IL-10 KO mice (Fig. 7B), supporting that phagocytic activity was enhanced. Furthermore, the ischemia-induced mRNA expression of typical anti-inflammatory M2 phenotype markers of myeloid cells, YM1 and arginase-1, was also significantly higher in the IL-10 KO mice (Fig. 7B).

Neutrophils (CD11b+Ly6G+) were detected in the ipsilateral cortex to a similar extent in IL-10 KO mice than in the WT (Fig. 7C). However, again the phenotype of these cells shifted in IL-10 KO mice since more Ly6G^{High} cells were detected in the latter group. Ly6G^{High} and F4/80^{High} cells described above were only found in the ischemic cortex, particularly in IL-10 KO mice, but were not detected in the blood of IL-10 KO or WT mice (not shown) suggesting that this phenotypic shift was induced by the local ischemic brain environment.

IL-10 is important for the immunosuppressive function of regulatory T cells (Treg). For this reason we examined whether IL-10 deficiency could alter the expression of other T cell immunosuppressive molecules. Notably, the ischemic tissue of IL-10 KO mice showed a significantly higher expression of the T cell inhibitory molecule CTLA-4 mRNA at day 4 post-ischemia compared to the WT ischemic tissue (Fig. 7B). In the spleen, similar percentages of Treg (CD3+CD4+CD25+Foxp3+) were detected in both genotypes 4 and 7 days post-ischemia (Supplementary Fig. 5). The proportion of CD3+CD4+CD25+ cells that were CTLA-4 (CD152) positive tended to increase in the spleen of IL-10 KO mice, but

differences versus the WT were not statistically significant (Supplementary Fig. 5). However, the CTLA-4 mean fluorescence intensity (MFI) in the CD3+CD4+CD25+ cell population (Fig. 7D), was significantly higher in the spleen of IL-10 KO mice 4 and 7 days post-ischemia (two-way ANOVA by genotype and time showed a significant genotype effect, $p<0.05$) (Fig. 7E), suggesting up-regulation of CTLA-4 expression in the Treg population of IL-10 deficient mice. Altogether these findings support that in the absence of IL-10 compensatory alternative immunosuppressive mechanism are up-regulated after stroke.

DISCUSSION

The results of this study show that IL-10 deficiency exacerbates brain inflammation after pMCAO, especially at day 4 when IL-10 is expected to exert an action in the ischemic tissue due to the up-regulation of this cytokine and its receptor. Strategies increasing anti-inflammatory IL-10 in the brain are beneficial in experimental ischemia [12,13], and mice deficient in IL-10 showed more brain damage than WT mice after pMCAO [14]. Here we found that IL-10 KO mice had slightly larger infarct volumes and worse neurological deficits than the WT mice during the first few days post-ischemia. However, these differences were attenuated at day 7, when in this experimental stroke model the extent of the lesion had markedly regressed [21,22]. This finding supports that IL-10 is not required for the process of lesion involution.

Notably, the increase in infarct volume in IL-10 KO mice found in our study was quite small and it was milder than that previously reported [14]. These differences in scale might be attributable to the specific animal housing conditions. Exposure of IL-10 KO mice to

environmental pathogens when they were kept under conventional housing conditions triggered the development of apparent signs of colitis, while maintaining the animals in a pathogen-free environment prevented this effect, as previously reported [16]. Development of colitis was associated with a worse stroke outcome, in agreement with the described worsening effect of systemic inflammation [20]. Therefore, ongoing inflammatory pathology adds a confounding factor exaggerating the direct effects of IL-10 deficiency in stroke.

IL-10 expression was up-regulated in the ischemic tissue soon after pMCAO, suggesting the involvement of resident cells. The capacity of microglia to secrete IL-10 has been reported after exposure to several agents such as adenosine [26], extracellular ATP [27], or LPS [28]. Several lines of evidence support beneficial functions for microglia in stroke [29, 30] but it is unknown whether these effects are dependent on IL-10. Treatment of cultured microglia with recombinant IL-10 did not attenuate the inflammatory reaction triggered by insufficient oxygen supply, but it strongly suppressed cytokine induction after TLR-4 activation. After brain ischemia, the initial inflammatory reaction can be secondarily aggravated by necrotic cell death, as it generates danger signals [31] that activate TLR-4, inducing further inflammation [8] and contributing to brain damage [32]. Here, IL-10 deficiency did not increase the local inflammatory reaction within the first hours following pMCAO, but it did 4 days later. This finding is in accordance with the exacerbated secondary inflammatory process seen in IL-10 KO mice after spinal cord compression injury [33] and in a model of brain bacterial infection [34].

The neuroinflammatory reaction is a dynamic process and inflammation is also involved in tissue repair mechanisms that are modulated by the complex crosstalk between resident glia and infiltrated immune cells [35]. Importantly, appropriate orchestration of

the inflammatory responses is critical to allow for lesion resolution. Reactive astrocytes can sense the presence of IL-10 since they showed strong expression of IL-10R at days 4 and 7 post-ischemia. Therefore, astrocytes may play a role in controlling inflammatory and immune responses after stroke. Infiltrated macrophages participate through phagocytosis in the process of clearance of the injured tissue [36]. In our experimental conditions, absence of IL-10 facilitated the presence in the ischemic tissue of myeloid cells ($F4/80^{High}$ cells) that are considered mature phagocytic cells. Accordingly, the ischemic tissue of IL-10 KO mice showed higher expression of galectin-3, a protein related to phagocytic activity, and greater up-regulation of the anti-inflammatory M2 makers arginase-1 and YM-1, compared to the WT mice. Neutrophils also acquired a more mature phenotype in the brain of IL-10 KO mice by showing higher expression of Ly6G. Neutrophils with this phenotypic feature have been described in the context of tumours [37] and in bacterial infections [38], where they exert anti-inflammatory and immunosuppressive functions. Since leukocytes with these features were not detected in the circulation, it is likely that the specific local brain environment was the trigger of the phenotypic changes observed in myeloid cells in the ischemic IL-10 KO brain.

Beneficial effects of Treg in brain ischemia are mediated by IL-10 [39]. Therefore, lack of IL-10 could impair the immunosuppressive function of Treg. However, immunosuppressive functions can be promoted by alternative mechanisms, such as that mediated by the T cell inhibitory receptor CTLA-4 [40], which after brain ischemia was more prominent in the IL-10 KO mice than in the WT.

In summary, this study shows that IL-10 attenuates the local inflammatory reaction after brain ischemia as IL-10 deficiency transiently enhanced the expression of pro-inflammatory cytokines and chemokines and slightly increased the size of the lesion and

worsened the neurological deficits. However, the study does not support a fundamental role for IL-10 in subsequent lesion involution, likely due to compensatory mechanisms able to control immune responses in the absence of IL-10.

Supplementary information is available at the Journal of Cerebral Blood Flow & Metabolism website – www.nature.com/jcbfm

ACKNOWLEDGEMENT

We thank Ms. Francisca Ruiz for excellent technical assistance, Dr. Tomàs Santalucia for advice on genotyping protocols, and Dr. Vanessa Brait for helpful comments. We are indebted to the Image and Cytometry platforms of the Institut d'Investigacions Biomèdiques August Pi i Sunyer (IDIBAPS) for technical help.

SOURCES OF FUNDING

Work supported by the Spanish Ministry of Economy (SAF2011-30492), and the European Community (FP7, grant agreements: n°201024 ARISE and n°278850 InMiND), and the ERANET-NEURON project (PRI-PIMNEU-2011-1342). IPP and EBT had PhD fellowships from *the Agència de Gestió d'Ajuts Universitaris i de Recerca* (AGAUR) of the *Generalitat de Catalunya* and the FPU program of the Spanish Ministry of Economy, respectively.

DISCLOSURES

The authors declare no disclosures.

REFERENCES

1. Lee JW, Bae SH, Jeong JW, Kim SH, Kim KW. Hypoxia-inducible factor (HIF-1)alpha: its protein stability and biological functions. *Exp Mol Med* 2004; 36: 1-12.

2. Geiger K, Leiherer A, Muendlein A, Stark N, Geller-Rhomberg S, Saely CH, *et al.* Identification of hypoxia-induced genes in human SGBS adipocytes by microarray analysis. *PLoS One* 2011; 6: e26465.

3. Li F, Wang L, Li JW, Gong M, He L, Feng R, *et al*. Hypoxia induced amoeboid microglial cell activation in postnatal rat brain is mediated by ATP receptor P2X4. *BMC Neurosci* 2011; 12: 111.

4. Feinman R, Deitch EA, Watkins AC, Abungu B, Colorado I, Kannan KB, *et al*. HIF-1 mediates pathogenic inflammatory responses to intestinal ischemia-reperfusion injury. *Am J Physiol Gastrointest Liver Physiol* 2010; 299: G833-843.

5. Kim SY, Choi YJ, Joung SM, Lee BH, Jung YS, Lee JY. Hypoxic stress up-regulates the expression of Toll-like receptor 4 in macrophages via hypoxia-inducible factor. *Immunology* 2010; 129: 516-524.

6. Tafani M, Schito L, Pellegrini L, Villanova L, Marfe G, Anwar T, *et al*. Hypoxia-increased RAGE and P2X7R expression regulates tumor cell invasion through phosphorylation of Erk1/2 and Akt and nuclear translocation of NF-{kappa}B. *Carcinogenesis* 2011; 32: 1167-1175.

7. Johnson GB, Brunn GJ, Platt JL. Activation of mammalian Toll-like receptors by endogenous agonists. *Crit Rev Immunol* 2003; 23: 15-44.

8. Gorina R, Font-Nieves M, Marquez-Kisinousky L, Santalucia T, Planas AM. Astrocyte TLR4 activation induces a proinflammatory environment through the interplay between MyD88-dependent NFκB signaling, MAPK and Jak1/Stat1 pathways. *Glia* 2011; 59: 242-255.

9. Block ML, Zecca L, Hong JS. Microglia-mediated neurotoxicity: uncovering the molecular mechanisms. *Nat Rev Neurosci* 2007; 8: 57-69.

10. Amantea D, Nappi G, Bernardi G, Bagetta G, Corasaniti MT. Post-ischemic brain damage: pathophysiology and role of inflammatory mediators. *FEBS J* 2009; 276: 13-26.

11. Serhan CN, Savill J. Resolution of inflammation: the beginning programs the end. *Nat Immunol* 2005; 6: 1191-1197.

12. de Bilbao F, Arsenijevic D, Moll T, Garcia-Gabay I, Vallet P, Langhans W, *et al*. In vivo over-expression of interleukin-10 increases resistance to focal brain ischemia in mice. *J Neurochem* 2009; 110: 12-22.

13. Ooboshi H, Ibayashi S, Shichita T, Kumai Y, Takada J, Ago T, *et al*. Postischemic gene transfer of interleukin-10 protects against both focal and global brain ischemia. *Circulation* 2005; 111: 913-919.

14. Grilli M, Barbieri I, Basudev H, Brusa R, Casati C, Lozza G, *et al*. Interleukin-10 modulates neuronal threshold of vulnerability to ischaemic damage. *Eur J Neurosci* 2000; 12: 2265-2272.

15. Vila N, Castillo J, Dávalos A, Esteve A, Planas AM, Chamorro A. Levels of anti-inflammatory cytokines and neurological worsening in acute ischemic stroke. *Stroke* 2003; 34: 671-675.

16. Kullberg MC, Ward JM, Gorelick PL, Caspar P, Hieny S, Cheever A, *et al*. Helicobacter hepaticus triggers colitis in specific-pathogen-free interleukin-10 (IL-10)-deficient mice through an IL-12- and gamma interferon-dependent mechanism. *Infect Immun* 1998; 66: 5157-5166.

17. Bouet V, Boulouard M, Toutain J, Divoux D, Bernaudin M, Schumann-Bard P, *et al*. The adhesive removal test: a sensitive method to assess sensorimotor deficicts in mice. *Nature Prot* 2009; 4: 1560-1564.

18. Cardona AE, Sasse ME, Liu L, Cardona SM, Mizutani M, Savarin C, *et al*. Scavenging roles of chemokine receptors: chemokine receptor deficiency is associated with increased levels of ligand in circulation and tissues. *Blood* 2008; 112: 256-263.

19. Li HL, Kostulas N, Huang YM, Xiao BG, van der Meide P, Kostulas V, *et al.* IL-17 and IFN-gamma mRNA expression is increased in the brain and systemically after permanent middle cerebral artery occlusion in the rat. J Neuroimmunol 2001; 116: 5-14.

20. McColl BW, Rothwell NJ, Allan SM. Systemic inflammatory stimulus potentiates the acute phase and CXC chemokine responses to experimental stroke and exacerbates brain damage via interleukin-1- and neutrophil-dependent mechanisms. *J Neurosci* 2007; 27: 4403-4412.

21. Henrich-Noack P, Baldauf K, Reiser G, Reymann KG. Pattern of time-dependent reduction of histologically determined infarct volume after focal ischaemia in mice. *Neurosci Lett* 2008; 432: 141-145.

22. Pialat JB, Cho TH, Beuf O, Joye E, Moucharrafie S, Langlois JB, *et al*. MRI monitoring of focal cerebral ischemia in peroxisome proliferator-activated receptor (PPAR)-deficient mice. *NMR Biomed* 2007; 20: 335-342.

23. Cervera A, Planas AM, Justicia C, Urra X, Jensenius JC, Torres F, *et al.* Genetically-defined deficiency of mannose-binding lectin is associated with protection after experimental stroke in mice and outcome in human stroke. PLoS One 2010; 5:e8433.

24. Lambertsen KL, Biber K, Finsen B. Inflammatory cytokines in experimental and human stroke. *J Cereb Blood Flow Metab* 2012; 32: 1677-1698.

25. Iwama A, Wang MH, Yamaguchi N, Ohno N, Okano K, Sudo T, *et al*. Terminal differentiation of murine resident peritoneal macrophages is characterized by expression of the STK protein tyrosine kinase, a receptor for macrophage-stimulating protein. *Blood* 1995; 86: 3394-3403.

26. Koscsó B, Csóka B, Selmeczy Z, Himer L, Pacher P, Virág L, *et al*. Adenosine augments IL-10 production by microglial cells through an A2B adenosine receptor-mediated process. *J Immunol* 2012; 188: 445-453.

27. Seo DR, Kim SY, Kim KY, Lee HG, Moon JH, Lee JS, *et al*. Cross talk between P2 purinergic receptors modulates extracellular ATP-mediated interleukin-10 production in rat microglial cells. *Exp Mol Med* 2008; 40: 19-26.

28. Ledeboer A, Brevé JJ, Wierinckx A, van der Jagt S, Bristow AF, Leysen JE, *et al*. Expression and regulation of interleukin-10 and interleukin-10 receptor in rat astroglial and microglial cells. *Eur J Neurosci* 2002; 16: 1175-1185.

29. Lalancette-Hébert M, Gowing G, Simard A, Weng YC, Kriz J. Selective ablation of proliferating microglial cells exacerbates ischemic injury in the brain. *J Neurosci* 2007; 27: 2596-2605.

30. Faustino JV, Wang X, Johnson CE, Klibanov A, Derugin N, Wendland MF, *et al*. Microglial cells contribute to endogenous brain defenses after acute neonatal focal stroke. *J Neurosci* 2011; 31: 12992-13001.

31. Harris HE, Raucci A. Alarmin(g) news about danger: workshop on innate danger signals and HMGB1. *EMBO Rep* 2006; 7: 774-778.

32. Caso JR, Pradillo JM, Hurtado O, Lorenzo P, Moro MA, Lizasoain I. Toll-like receptor 4 is involved in brain damage and inflammation after experimental stroke. *Circulation* 2007; 115: 1599-1608.

33. Genovese T, Esposito E, Mazzon E, Di Paola R, Caminiti R, Bramanti P, *et al*. Absence of endogenous interleukin-10 enhances secondary inflammatory process after spinal cord compression injury in mice*. J Neurochem* 2009; 108: 1360-1372.

34. Deckert M, Soltek S, Geginat G, Lütjen S, Montesinos-Rongen M, Hof H, *et al*. Endogenous interleukin-10 is required for prevention of a hyperinflammatory intracerebral immune response in Listeria monocytogenes meningoencephalitis. *Infect Immun* 2001; 69: 4561-4571.

35. Ransohoff RM, Brown MA. Innate immunity in the central nervous system. *J Clin Invest* 2012; 122: 1164-1171.

36. Schwartz M. Tissue-repairing" blood-derived macrophages are essential for healing of the injured spinal cord: From skin-activated macrophages to infiltrating blood-derived cells? *Brain, Behavior, and Immunity* 2010; 24: 1054–1057.

37. Zoglmeier C, Bauer H, Nörenberg D, Wedekind G, Bittner P, Sandholzer N, *et al*. CpG blocks immunosuppression by myeloid-derived suppressor cells in tumor-bearing mice. *Clin Cancer Res* 2011; 17: 1765-1775.

38. Zhang X, Majlessi L, Deriaud E, Leclerc C, Lo-Man R. Coactivation of Syk kinase and MyD88 adaptor protein pathways by bacteria promotes regulatory properties of neutrophils. *Immunity* 2009; 31: 761-771.

39. Liesz A, Suri-Payer E, Veltkamp C, Doerr H, Sommer C, Rivest S*, et al*. Regulatory T cells are key cerebroprotective immunomodulators in acute experimental stroke. *Nat Med* 2009;15:192-199.

40. Ertelt JM, Buyukbasaran EZ, Jiang TT, Rowe JH, Xin L, Way SS. B7-1/B7-2 blockade overrides the activation of protective CD8 T cells stimulated in the absence of Foxp3+ regulatory T cells. *J Leukoc Biol*. 2013 Jun 6. [Epub ahead of print]

Titles and legends to figures

Fig. 1 *Ischemia up-regulates the expression of IL-10 and IL-10 receptor in WT mice.* A) Expression of IL-10 mRNA progressively increases in brain tissue after pMCAO from 6 hours (h) to 7 days (d). B) The extent of IL-10 mRNA expression correlates (linear regression analysis, $p<0.03$) with infarct volume that was measured by MRI (T2) in the same animals 6 hours following pMCAO. C) The concentration of soluble IL-10 in brain tissue increased after pMCAO. D) Increased expression of IL-10 receptor (IL-10R) is apparent from 4 days post-ischemia, but not within the first day. mRNA values are expressed as fold increase versus control non-ischemic brain tissue, and protein values are expressed as pg of IL-10 per mg of brain protein. E-H) Immunofluorescence staining of IL-10R (green) in the cortex of controls (E) and after pMCAO (F-H). E) IL-10R immunoreaction (green) is not detected in the control cortex. Isolectin (red) staining shows resident microglia and blood vessels. F) Isolated IL-10R positive cells are detected in the subarachnoid space on the top of the ischemic cortex after pMCAO. G) IL-10R immunoreactive cells (green) are seen in superficial cortical layers from 4 days post-ischemia. These cells are rarely positive (arrow) for isolectin (red) and most of the IL-10R+ cells have morphology (arrowhead) compatible with that of reactive astrocytes. H) Double-staining with GFAP (red) shows that most IL-10R+ cells are astrocytes (arrow). The cell nuclei were stained with Hoechst (blue). Images in F, G and H correspond to days 1, 4 and 7 after pMCAO, respectively. Bar scale: 20 μm. n=4-6 mice per group. * $p<0.05$, *** $p<0.001$.

Fig. 2 *IL-10 deficiency slightly increases infarct volume and neurological deficits.* A) Brain infarction was longitudinally monitored by T2 MRI in the same mice at days 1, 4 and 7 post-ischemia and a representative animal per group is shown. B) Infarct volume is

slightly larger in IL-10 KO mice (n=17) than in the WT (n=20) (two-way ANOVA by genotype and time; $p<0.05$ for genotype effect; $p<0.001$ for time effect). C) In an additional group of mice, MRI was followed by histology in the same mice. T2 maps of representative brain slices at day 7 after pMCAO are shown with their corresponding histological staining (cresyl violet). D) Infarct volume measured by MRI and by histological means in the same mice shows a good correlation (linear regression analysis, $r^2=0.8$, $p<0.001$). E) The infarct volume measured by histological means is significantly smaller ($p<0.001$) than the corresponding MRI measures. However, with either method, genotype group differences at day 7 are not statistically significant. F) At day 1, the ratio of the volume of the ipsilateral to the contralateral hemisphere is above 1 due to edema. The effect is attenuated at day 4, while at day 7 the ipsilateral hemispheric volume is reduced. However hemispheric volume differences between WT and IL-10 KO mice are similar along time. D-F) Measure of the time to shake (D), contact (E) and remove (F) steps of the adhesion/removal tape test shows worse neurological deficits at day 3, as shown by a significant delay in the time to shake (D) and remove (F) for the contralateral (left) forepaw, but the worsening effects of IL-10 deficiency are attenuated at day 7. Animals in panels (F-I) are the same as in (B) * $p<0.05$.

Fig. 3 *IL-10 deficiency does not exacerbate the inflammatory reaction 6 hours post-ischemia.* The mRNA expression for the stated molecules increases in both WT and IL-10 KO ischemic brain tissue at 6 hours. Values are expressed as fold versus control WT. n=6 mice per group, * $p<0.05$, ** $p<0.01$.

Fig. 4 *In cultured microglia, IL-10 attenuates the inflammatory response to LPS but not that induced by exposure to ischemic conditions.* Cultured microglia show selective

inflammatory responses after stimulation with either 3-hour anoxia (group '*A'*) or with 10 ng/mL LPS (group '*LPS'*). A-F) Cytokine mRNA expression was evaluated by qRT-PCR analysis 6 hours after initiation of the challenge. G-J) Cytokine concentration in the culture medium was measured also at 6 hours by ELISA assays. A, C, E, G, I) Treatment with recombinant murine IL-10 (10 ng/mL) does not attenuate the response to anoxia (group '*A+IL-10*'). B, D, F, H, J) However, IL-10 strongly prevents the inflammatory response to LPS (group '*LPS+IL-10*'). Values were obtained in three independent cultures. Symbol * refers to comparison versus control, and symbol & refers to comparison versus either anoxia or LPS. One symbol: $p<0.05$, two symbols: $p<0.01$, and three symbols: $p<0001$.

Fig. 5 *IL-10 deficiency exacerbates secondary inflammation at day 4 after pMCAO.* Brain expression of cytokine and chemokine mRNA is significantly increased in IL-10 KO than in WT mice at day 4, with the exception of CX3CL1, which decreases in IL-10 KO mice. Values are expressed as fold versus control WT. n=6 mice per group, * $p<0.05$, ** $p<0.01$, *** $p<0.001$.

Fig. 6 *Differences between WT and IL-10 KO mice in the brain inflammatory response are attenuated at day 7.* Brain expression of most cytokine and chemokine mRNA is no longer significantly different between IL-10 KO and WT mice at day 7. n=6 mice per group. Values are expressed as fold versus control WT. * $p<0.05$, ** $p<0.01$, *** $p<0.001$.

Fig. 7 *Compensatory immunosuppressive mechanisms in IL-10 KO mice after ischemia.* A) Ischemia increases the number of cells expressing F4/80+ (microglia/macrophages) to a similar extent in both genotypes at day 4. However, more F4/80^{High} phagocytic cells

are seen in the brain of IL-10 KO than in WT mice. B) The ischemic tissue of IL-10 KO mice shows a higher up-regulation of the mRNA of galectin-3, Arginase-1, YM-1 and CTLA-4 (n=4-6 samples per time group). C) At day 4, the numbers of Ly6G+ cells (neutrophils) is similar in the ipsilateral cortex of IL-10 KO and WT mice, but higher numbers of $Ly6G^{High}$ neutrophils are seen in the ischemic cortex of the IL-10 KO mice. Flow cytometry diagrams shown in the right panels of (A) and (C) correspond to one representative sample out of n=5 independent samples per group. D) Representative dot plots of CTLA-4 expression (CD152) in splenocytes from WT mice and IL-10 KO mice 7 days after pMCAO. Single viable cells are plotted by CD152 versus CD4 expression. E) Single viable splenocytes are subsequently gated on CD3+ CD4+ and CD25+ cells. CTLA-4 mean fluorescence intensity (MFI) in the latter cells is higher in IL-10 KO mice than in WT mice. Two-way ANOVA by genotype and time. *$p<0.05$ and ***$p<0.001$ versus ischemic tissue of WT mice.

Figure 1

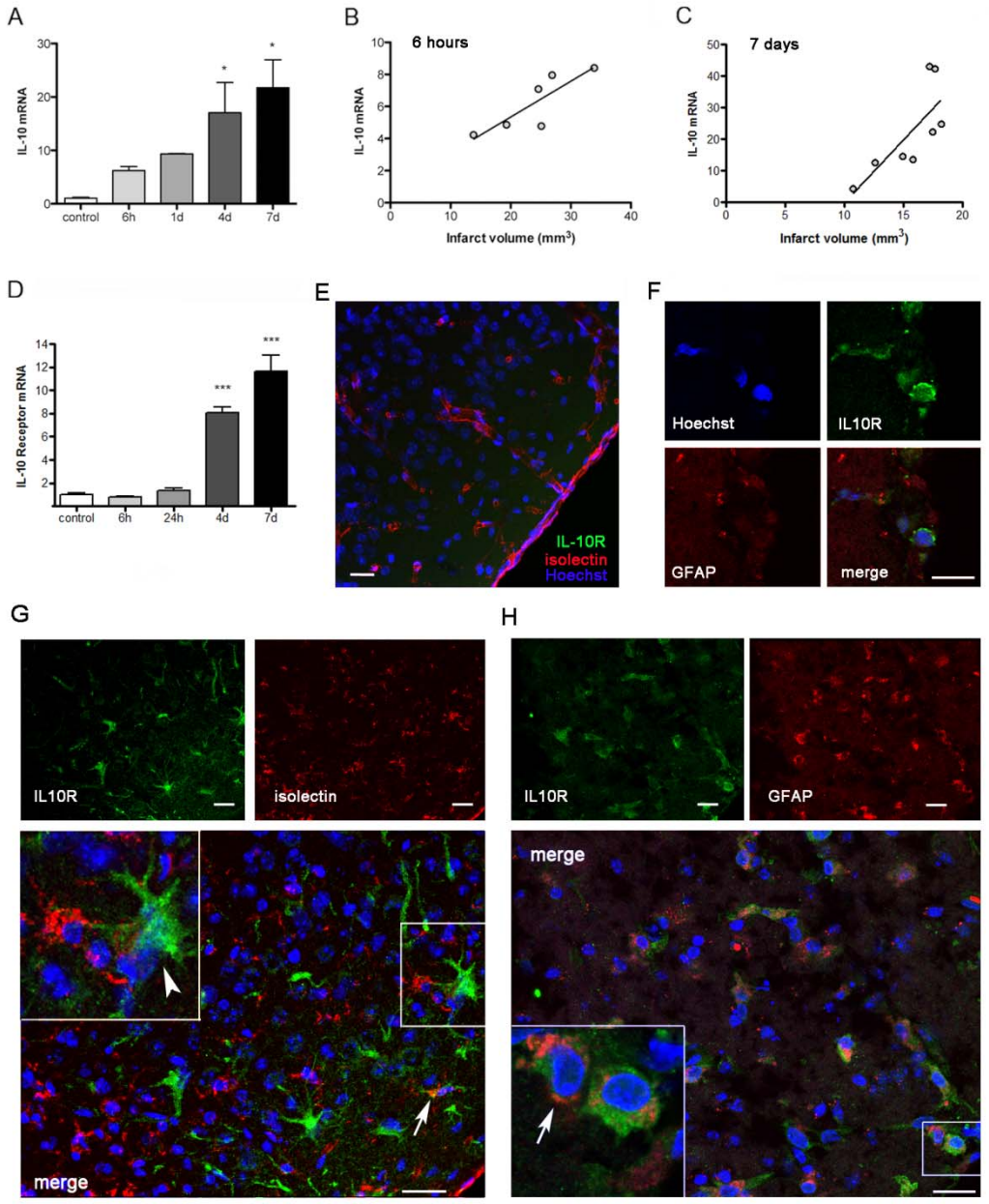
A
IL-10 mRNA
control
6h
1d
4d
7d
B
6 hours
IL-10 mRNA
Infarct volume (mm3)
C
7 days
IL-10 mRNA
Infarct volume (mm3)
D
IL-10 Receptor mRNA
control
6h
24h
4d
7d
E
IL-10R
isolectin
Hoechst
F
Hoechst
IL10R
GFAP
merge
G
IL10R
isolectin
merge
H
IL10R
GFAP
merge

Figure 2

Figure 2

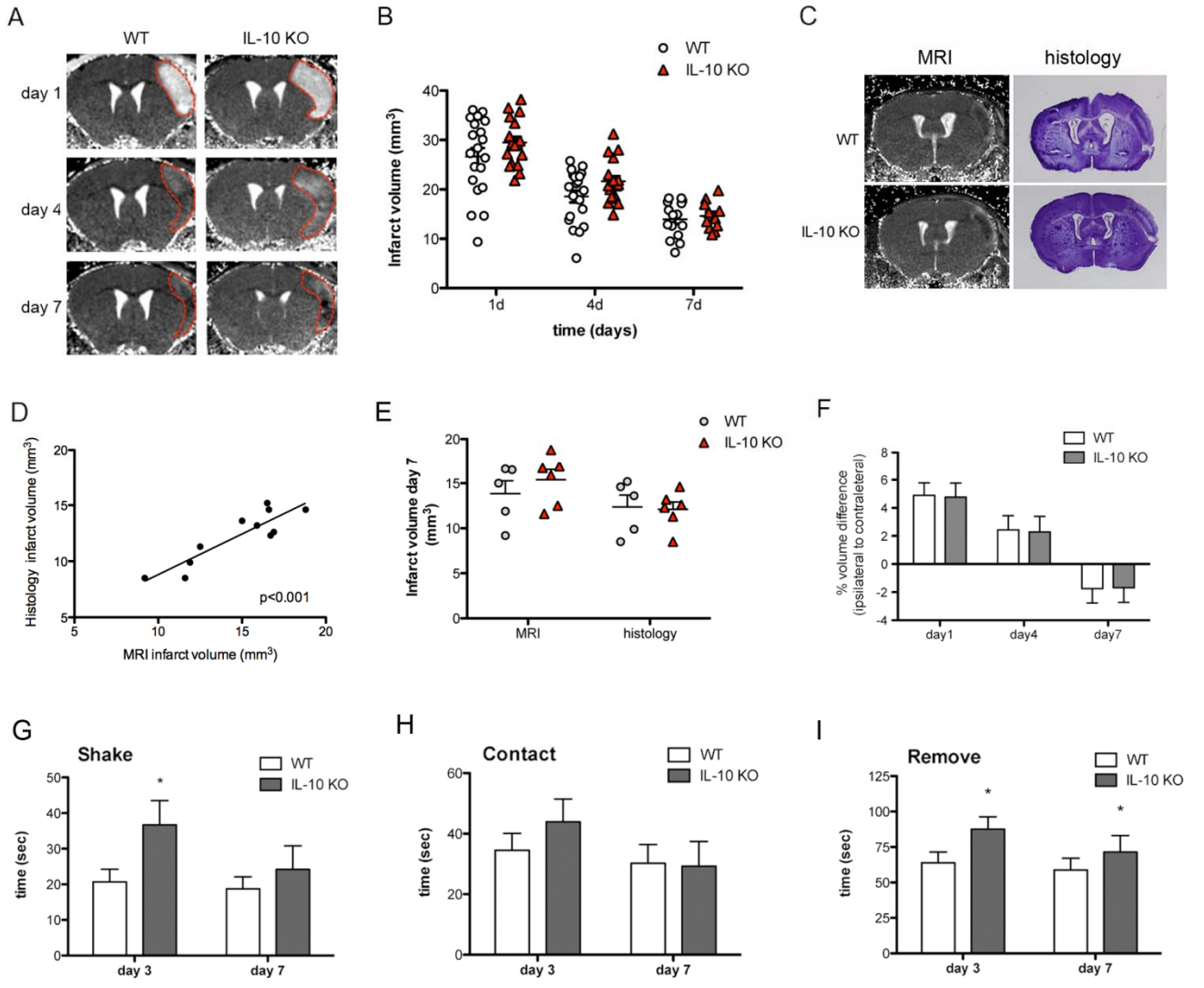

Figure 3

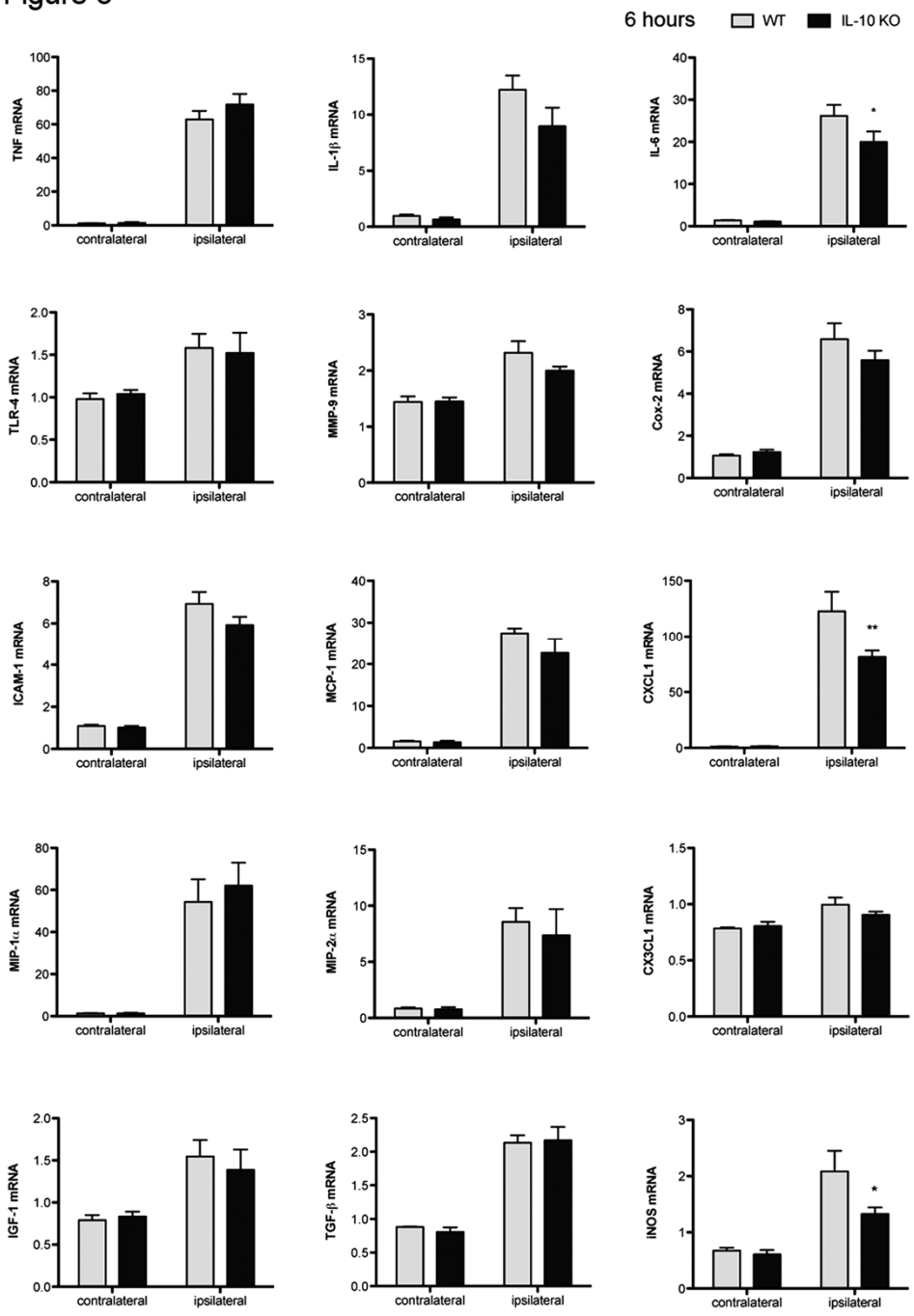
6 hours
WT
IL-10 KO
TNF mRNA
IL-1β mRNA
IL-6 mRNA
TLR-4 mRNA
MMP-9 mRNA
Cox-2 mRNA
ICAM-1 mRNA
MCP-1 mRNA
CXCL1 mRNA
MIP-1α mRNA
MIP-2α mRNA
CX3CL1 mRNA
IGF-1 mRNA
TGF-β mRNA
iNOS mRNA
contralateral
ipsilateral
*
**

Figure 4

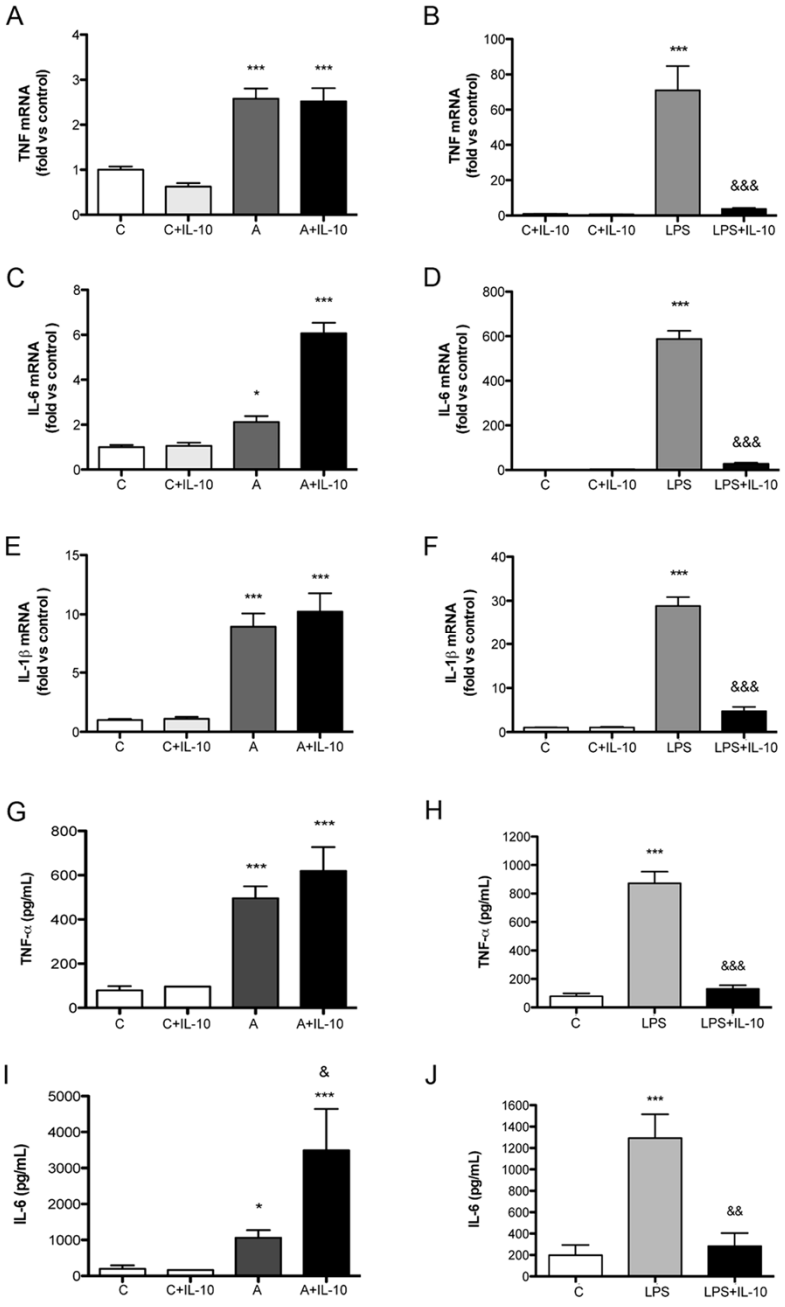
A
TNF mRNA (fold vs control)
C
C+IL-10
A
A+IL-10
***
B
TNF mRNA (fold vs control)
C+IL-10
LPS
LPS+IL-10
***
&&&
C
IL-6 mRNA (fold vs control)
*
D
IL-6 mRNA (fold vs control)
E
IL-1β mRNA (fold vs control)
F
IL-1β mRNA (fold vs control)
G
TNF-α (pg/mL)
H
TNF-α (pg/mL)
I
IL-6 (pg/mL)
&
J
IL-6 (pg/mL)
&&

Figure 5

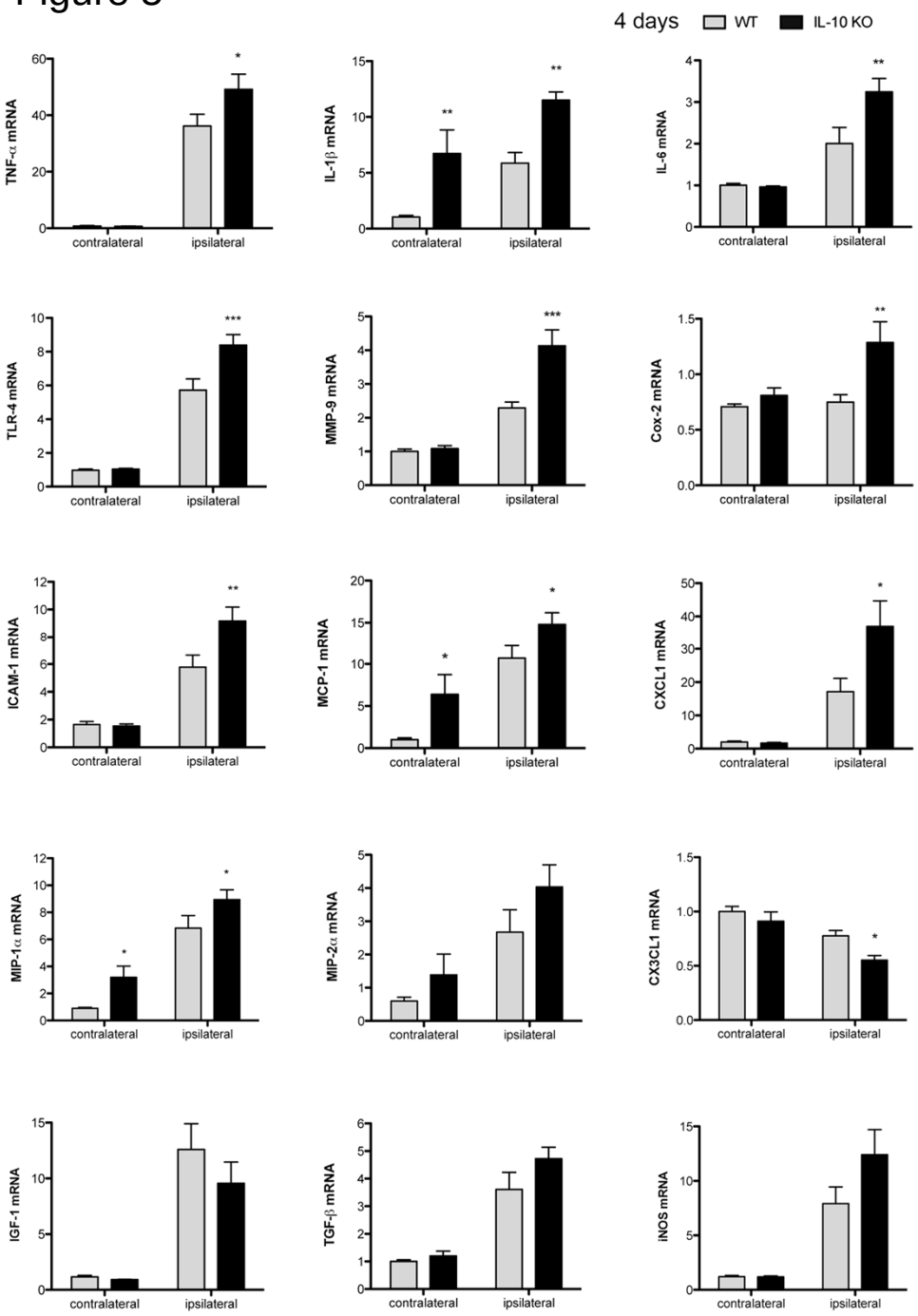
4 days
WT
IL-10 KO
TNF-α mRNA
IL-1β mRNA
IL-6 mRNA
TLR-4 mRNA
MMP-9 mRNA
Cox-2 mRNA
ICAM-1 mRNA
MCP-1 mRNA
CXCL1 mRNA
MIP-1α mRNA
MIP-2α mRNA
CX3CL1 mRNA
IGF-1 mRNA
TGF-β mRNA
iNOS mRNA
contralateral
ipsilateral

Figure 6

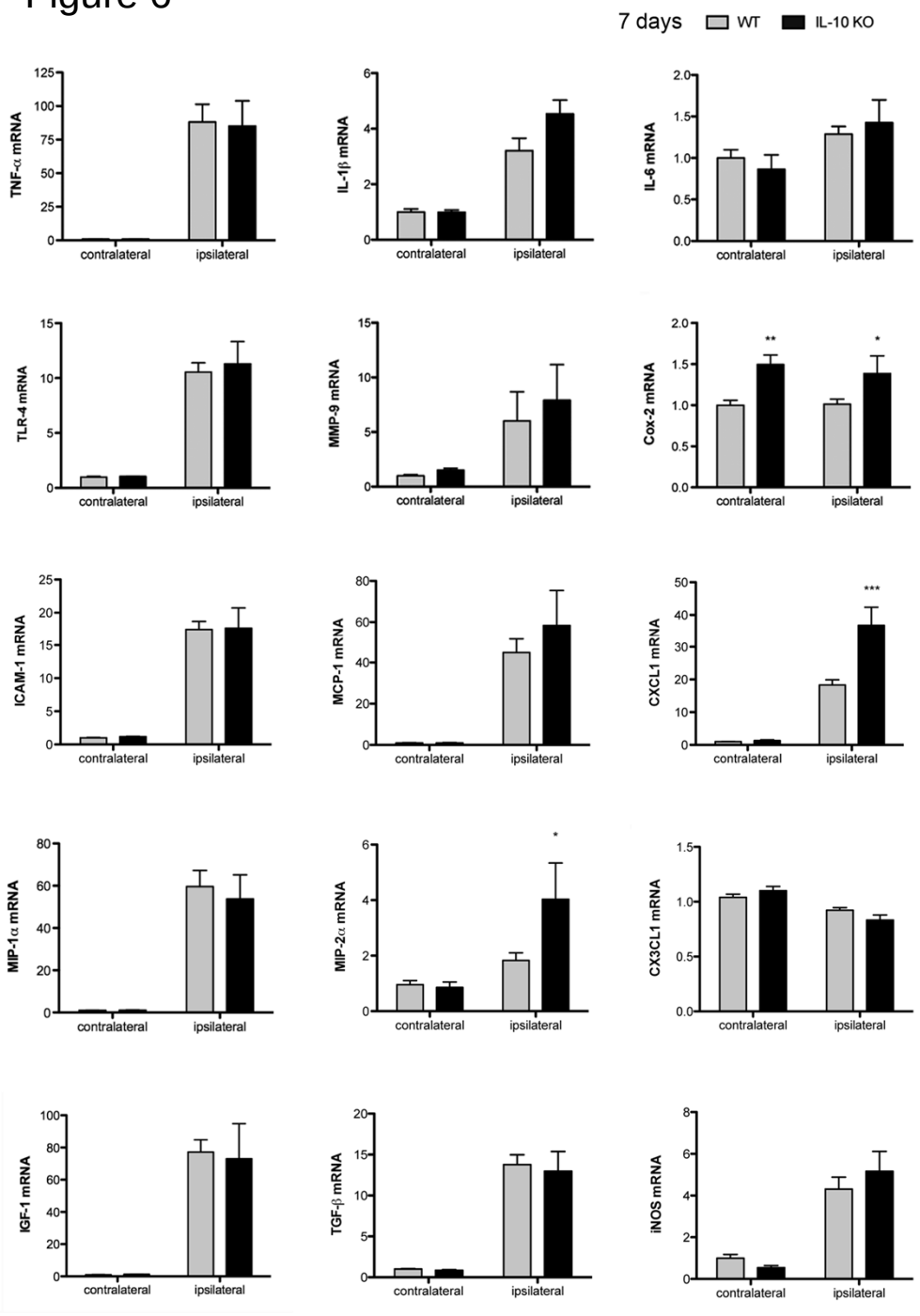
7 days
WT
IL-10 KO
TNF-α mRNA
IL-1β mRNA
IL-6 mRNA
TLR-4 mRNA
MMP-9 mRNA
Cox-2 mRNA
ICAM-1 mRNA
MCP-1 mRNA
CXCL1 mRNA
MIP-1α mRNA
MIP-2α mRNA
CX3CL1 mRNA
IGF-1 mRNA
TGF-β mRNA
iNOS mRNA
contralateral
ipsilateral
**
*
***

Figure 7

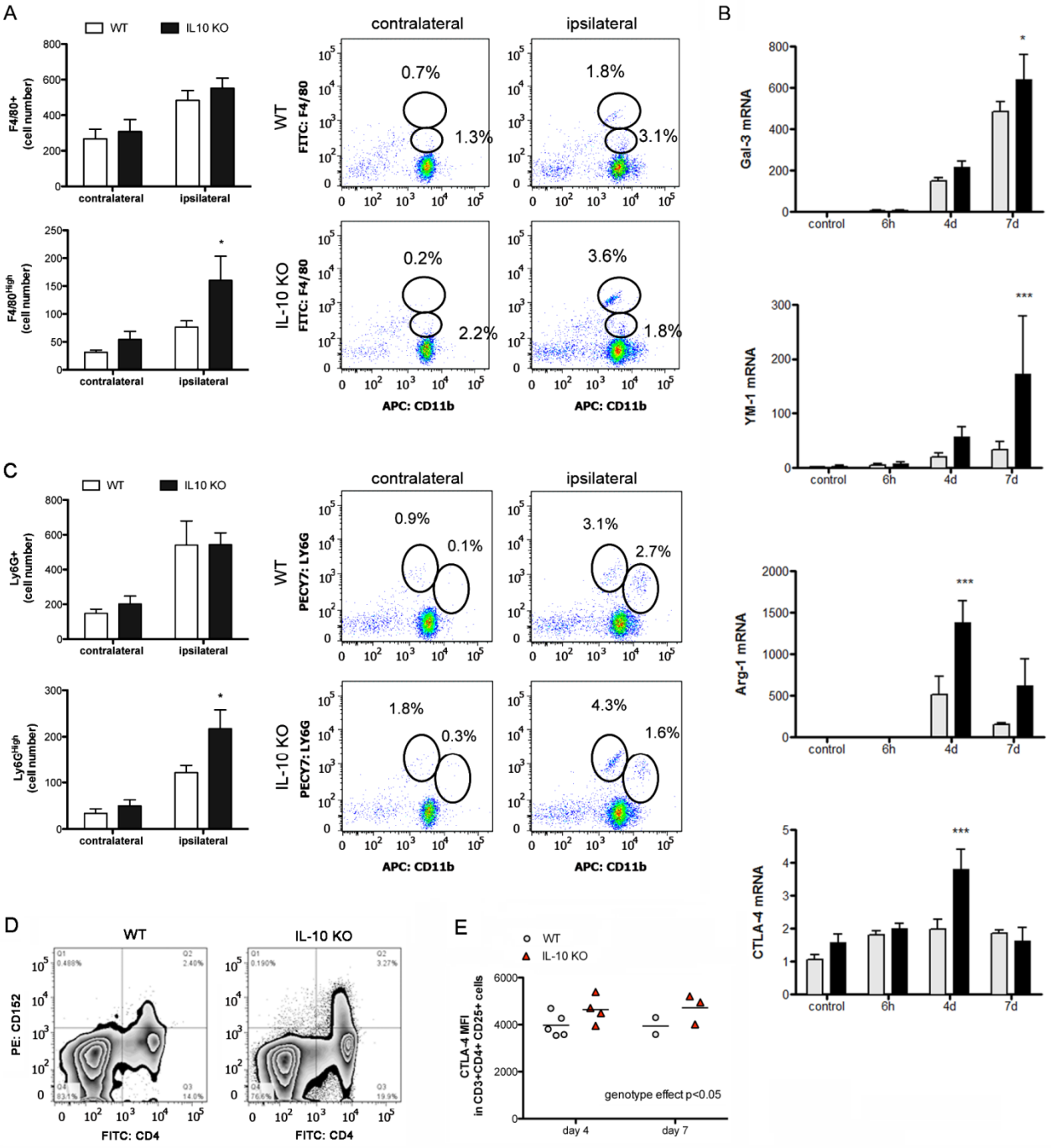
A
WT
IL10 KO
F4/80+ (cell number)
contralateral
ipsilateral
F4/80High (cell number)
contralateral
ipsilateral
contralateral
ipsilateral
WT
FITC: F4/80
0.7%
1.3%
1.8%
3.1%
IL-10 KO
FITC: F4/80
0.2%
2.2%
3.6%
1.8%
APC: CD11b
APC: CD11b
B
Gal-3 mRNA
control
6h
4d
7d
YM-1 mRNA
control
6h
4d
7d
Arg-1 mRNA
control
6h
4d
7d
CTLA-4 mRNA
control
6h
4d
7d
C
WT
IL10 KO
Ly6G+ (cell number)
contralateral
ipsilateral
Ly6GHigh (cell number)
contralateral
ipsilateral
contralateral
ipsilateral
WT
PECY7: LY6G
0.9%
0.1%
3.1%
2.7%
IL-10 KO
PECY7: LY6G
1.8%
0.3%
4.3%
1.6%
APC: CD11b
APC: CD11b
D
WT
IL-10 KO
PE: CD152
FITC: CD4
FITC: CD4
E
WT
IL-10 KO
CTLA-4 MFI in CD3+CD4+ CD25+ cells
genotype effect p<0.05
day 4
day 7

Supplementary Fig. 1: Cells were morphologically identified by forward and side scatter (FSC-A vs SSC-A) parameters. Viable cells were further analyzed by exclusion of doublets and by antigen positivity on CD11b, CD45, F4/80 and Ly6G.

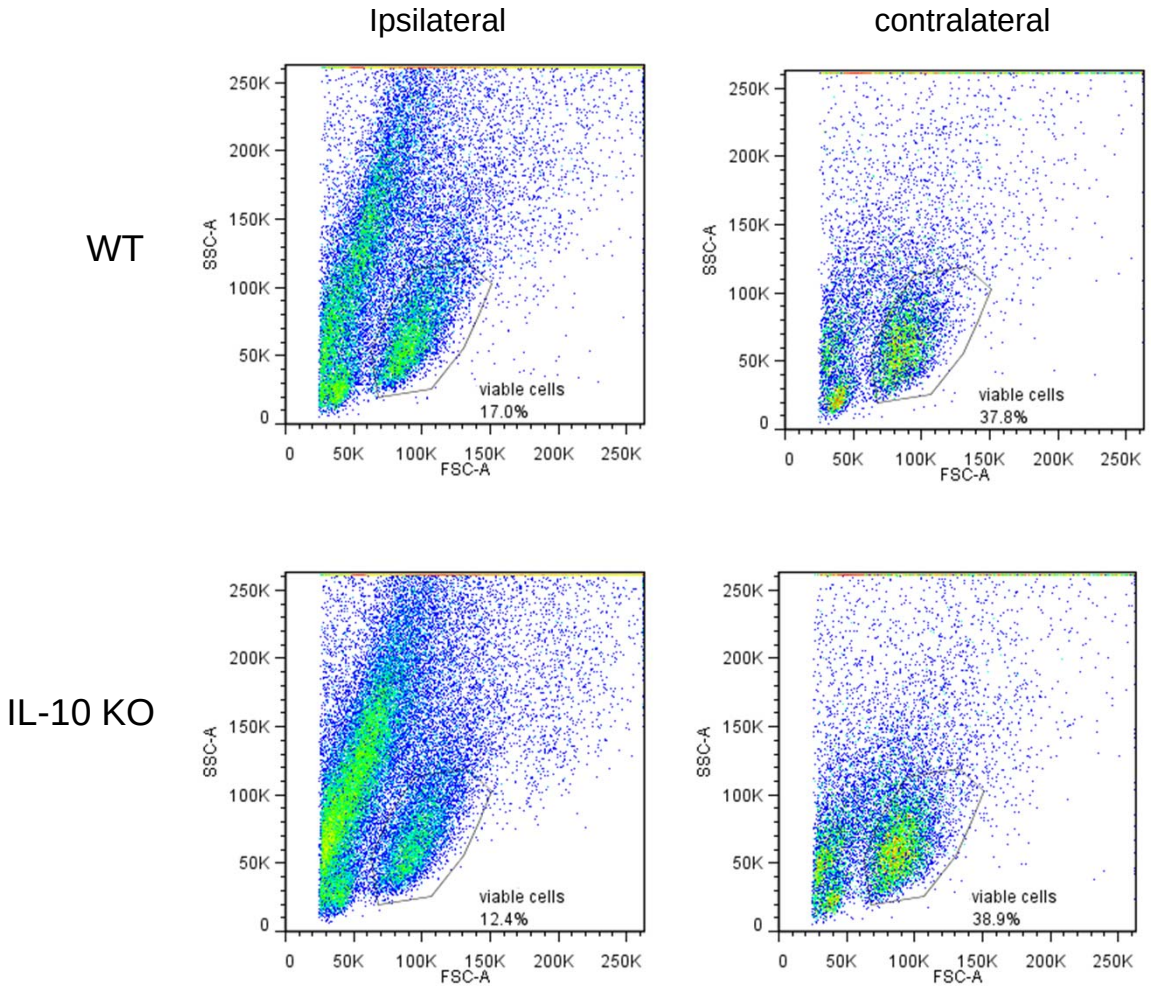

Supplementary Fig. 2

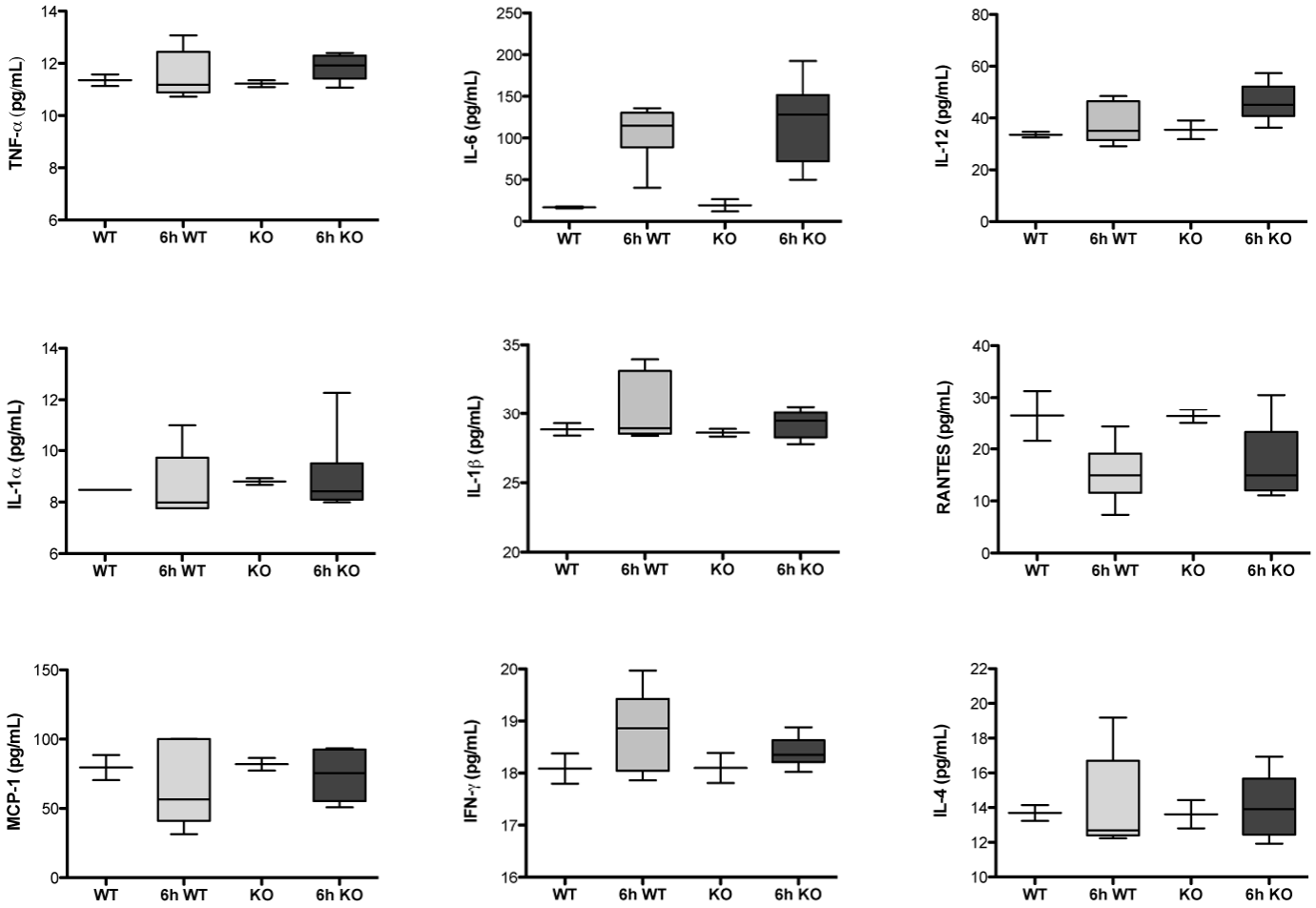

Supplementary Fig. 3

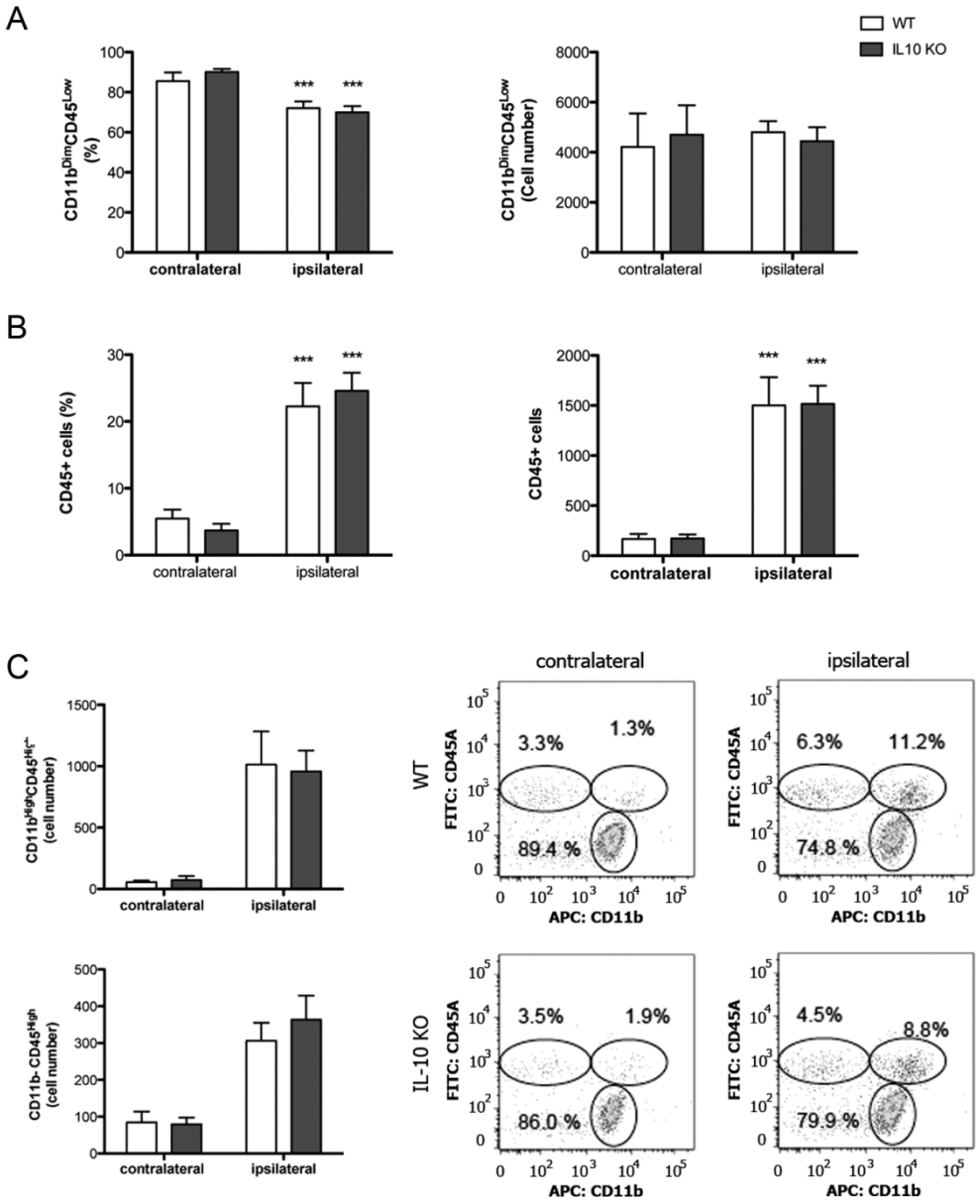

Supplementary Fig. 4